INTERSECTII
INTERSECTIONS
http://www.intersections.ro

A numerical study on the behaviour of eccentrically braced frames in seismic areas using finite element analysis

Adina Vătăman[1], Adrian Ciutina[1] and Daniel Grecea[1, 2]
[1]*Department of Steel Structures and Structural Mechanics, Politehnica University of Timişoara, 300224, Romania*
[2]*Romanian Academy Timişoara Branch, 300223, Romania*

Summary

Summary

Eccentrically braced frames are a common structural typology in areas with seismic activity due to seismic energy dissipation capacity by deformation of the dissipative "link". The presence of the dissipative element allows the frame to withstand large seismic lateral forces by facilitating the formation of a plastic hinge in the link. In the case of short links failure occurs through shear of the web panel, in the case of long links failure occurs in bending, and in the case of intermediate link lengths, there is a combined effect. The current study is focused on eccentrically braced frames with short steel link element. There are many parameters that can influence the behaviour of the link, such as its length and slenderness of the steel profile, the presence of intermediate stiffeners or the presence of the concrete slab with or without shear connectors.

The current numerical study analyses the behaviour of eccentrically braced frames (EBFs) in the case of seismic loading, based on previous experimental data. The calibration of the numerical model is done by means of FEM software Abaqus while subjecting the model to both monotonic and cyclic loading. Due to the complex nature of the problem, different modelling solutions are investigated and compared.

KEYWORDS: EBF, Steel, Link, FEM.

1. INTRODUCTION

In the case of seismic loading, the steel Eccentrically Braced Frames (EBF) represent structures recognized for their good dissipation capacities. Such systems are characterised design by high values of the behaviour factor (q greater than 6 in ductility class high case), the seismic energy being dissipated by the formation of plastic hinges in the link elements. They represent elements highly loaded in shear

ISSN 1582-3024

and/or bending, in the case of lateral loads resisted by the triangulated adjacent systems. The formation of a plastic hinge in the link element allows for the other frame components to remain in the elastic domain, thus achieving local failure rather than a global failure of the structure.

The general philosophy in the design of steel structures states that the main concern in the case of the ultimate limit state is the limitation of deformations, in order to avoid important second order effects and other instabilities [1]. However, the formation of the plastic mechanism is aimed by design, in such a way that the plastic hinges form in elements with ductile behaviour. Thus, the ductility of the dissipative zones became of high importance in such cases, in order to allow plastic redistribution of forces [2].

In accordance with the European seismic norm – Eurocode 8 [3], short links are defined by their length $e_s < 1.6(M_{pl}/V_{pl})$ [mm] and are subjected preponderantly to shear. As proven by other authors [4], the link elements behaviour is very ductile proving high values of distortion of the order 120 to 200 mrad. On the other hand, structural simulations [5] on structures subjected to dynamic incremental analyses with accelerograms have proven that the limiting value proposed by EC8-1, § 6.8.2., of 80 mrad for short links in EBF might be insufficient for structures in high seismicity zones. However, as proven by Degee et al [6], the short links (vertical in this case) can assure adequate global structural dissipation capacities, having behaviour factors q as high as 6. Considering the stiffening of the dissipative link working in shear, Yurisman et al. [7], based on experimental tests performed numerical simulations on links with diagonal web stiffeners, showing their improved capacity in resistance. The experimental study performed by Okazaki et al. [8] in function of several parameters affecting the disposition and general form of web stiffeners leads to interesting results regarding link flange slenderness and the importance of an appropriate loading protocol.

Unlike the simple definition of the short link elements offered by EN 1998-1, the above-mentioned studies show that other parameters can influence the dissipative capacities of eccentrically braced frames, such as different loading conditions, the presence of stiffeners on the link element web, the length of the element or the slenderness of the link profile. The current paper is aimed at presenting the calibration of an experimental model using finite element analysis in order to investigate the influence of such details on the overall response of EBF with short steel link elements.

INTERSECTII
INTERSECTIONS
http://www.intersections.ro

2. CALIBRATION OF NUMERICAL MODEL

2.1. Experimental Basis

A large experimental study was undertaken at the CEMSIG laboratory of the Politehnica University of Timisoara [9] concerning the behaviour of eccentrically braced frames with short link elements in different solutions (steel/composite) and with different loading patterns (monotonic/cyclic). The reference specimen for the study was a steel EBF with a fixed short link element, loaded monotonically, EBF-LF-M. This is also the specimen that was used for the numerical calibration.

The testing sub-assembly was part of a larger dual frame structure (moment resisting frames + eccentrically braced frames) with five storeys and three bays (outer bays of 6m and an inner bay of 4.5m). The design has taken the seismic zone of Bucharest into consideration, using the following design details: a_g = 0.24g, T_C = 1.6 sec; a permanent load of 4 kN/m^2 and a live load of 3 kN/m^2.

The reference EBF specimen (denoted as EBF-LF-M) represents the first storey central bay of this structure. The beam is an HE200A profile (including the link zone of 300mm), columns are HE260B profiles, and braces are HE180A profiles, as it can be distinguished in Figure 1a. Although not required by design, the beam-to-column joints were designed as full-resistant (extended end-plate bolted connections) in view of transmitting the axial load. The columns were pinned at the base in order to reduce the lateral force in the actuators, see Figure 1b) for loading lay-out.

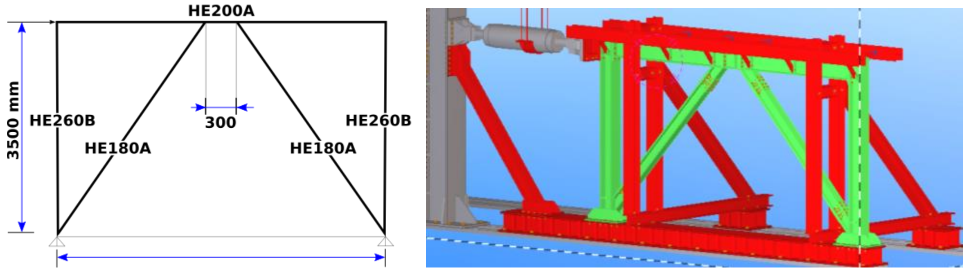

a) b)

Figure 1. a) Dimensions of the steel EBF specimen; b) Experimental lay-out

The loading of the sub-assembly was made using displacement control by means of a loading actuator placed at the top left corner of the frame on the column flange. The displacement of the frame was monitored by means of multiple displacement transducers. The maximum recorded displacement was 180mm and the testing procedure ended due to limitations of the technological equipment. The maximum displacement of 180 mm corresponds to a link rotation greater than 250 mrad, four times higher than the value mentioned in the norm (80 mrad in EN 1998-1). At maximum deflection, the web of the link suffered significant crippling due to shear force, as is shown in Figure 3d).

Figure 2a) shows the resulting force - lateral displacement curve, derived from the pushing load of the actuator and the lateral displacement of the left frame corner, monitored by means of a displacement transducer. Figure 2b) shows the derived V (shear force) – γ (distortion angle) curve of the link element, where V is computed according to the static schema of the frame and γ represents the distortion angle of the link web, computed on the basis of displacement transducers located on the link itself (diagonal on the web panel). It should be mentioned that for the configuration presented, only the dissipative area of the link element has undergone plastic deformations, all other elements such as braces, columns and beams within the triangulated zone, as well as their connections exhibited elastic behavior. However, noticeable deformation was recorded in the brace and brace connections up to 4mm per brace, due to sliding of the connection elements.

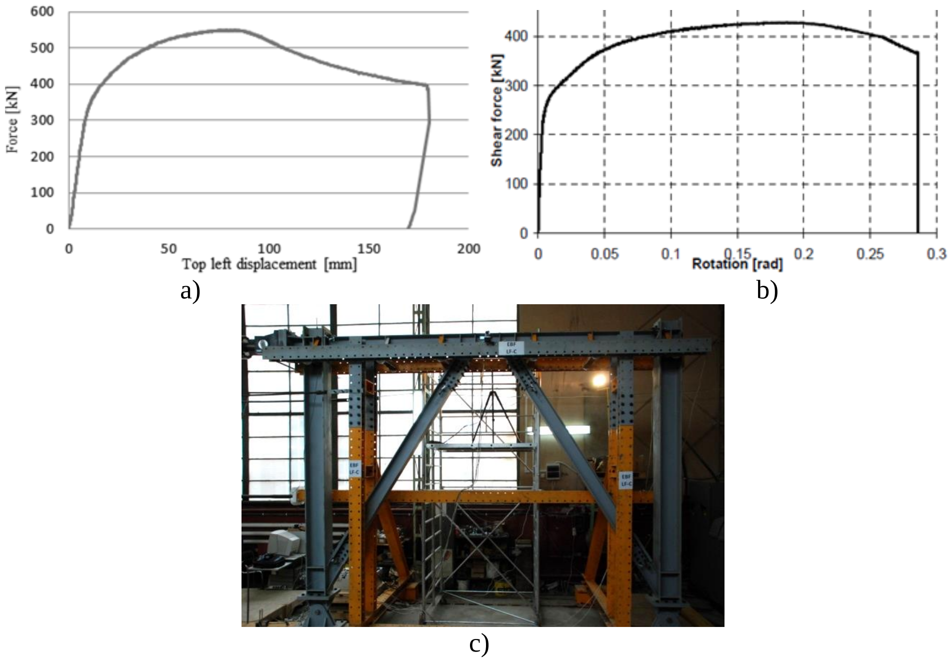

Figure 2. a) Force-displacement curve for steel EBF; b) Shear force-rotation curve of dissipative element; c) Experimental set-up

2.2. Finite element model and calibration

The numerical study which will be presented further was based on the initial experimental results. The numerical finite element model of the reference frame EBF-LF-M was created using finite element software ABAQUS 6.11-1 [10] by

ISSN 1582-3024

considering 3D solid frame elements, as shown in Figure 3. The model was assigned the name LS3-H0-M, corresponding to short steel link with the length of 300mm, with an H profile (HE200A) undergoing a monotonic loading procedure.

The model was assigned the same geometrical properties as the tested specimen. The link element was considered fixed as well and the column base connections were considered to be pinned connections. The assigned material properties were corresponding to nominal values of materials, in compliance with the specifications from Eurocode 3 Part 1-3 [11], considering the results of coupon tests (see Figure 3b), but transformed in true stress-strain curves in case of the beam, including dissipative link [12]. These true stress-strain material properties were assigned only for the beam because initial analyses were in accordance to experimental testing proving that the rest of the frame elements remained in the elastic domain.

The analysis procedure used was Dynamic Explicit with a monotonically applied displacement of 180 mm on the top of the left column, similar to the maximum recorded displacement for the corresponding displacement transducer in experimental testing.

Hex type C3D8R finite elements have been used for meshing using a sweep technique and mixed medial axis and advancing front algorithms. Different finite element sizes have been used. An element size of 6mm was used for the dissipative part of the frame (link element and adjacent beam ends) as shown in Figure 3a). The frame components, which were expected to remain in the elastic domain, were assigned larger size elements: 25mm for columns and column stiffeners, 20mm for beam and beam stiffeners and respectively 15mm for braces.

The resulting force-displacement curve (denoted as FEModel) followed the experimental response appropriately, as it could be observed in Figure 4a), however, the initial stiffness of the numerical model was slightly higher than that of the experimental model.

The displacement transducers recorded a slip of the bolted connections of the braces during experimental testing, so this was further integrated into the numerical model by a using a connector and a sliding element at the middle of the braces (Figure 4c). The connector was assigned a displacement law according to recorded values of elastic deformation considering a maximum 1.5mm slip at a force of 300kN. The finite element response corresponding to this situation is shown as curve FEModel+Slip in Figure 4 a).

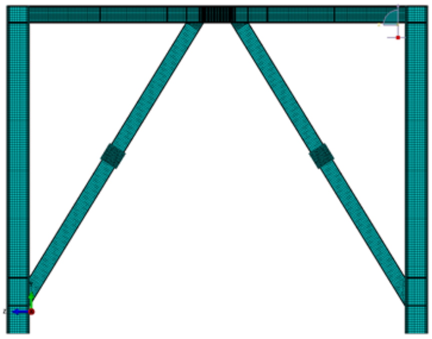

Element profile		Measured steel yield strength	Tensile strain at break
		[N/mm^2]	[%]
Beam web	HE200A	304	32.24
Beam Flange	HE200A	323	35.01
Column	HE260B	355	15
Brace	HE180A	355	15

b)

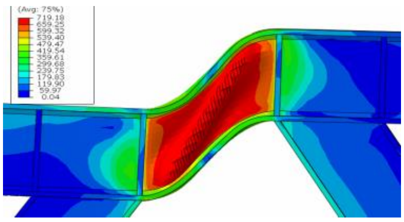

c)

d)

Figure 3. a) Mesh of the finite element EBF model; b) material characteristics used in calibration; The deformed shape of the dissipative link elements: c) FE Model d) Laboratory test

As this additional effect was shifting the maximum resistance point, adjustments on the applied constraints and boundary conditions were considered for re-fitting the experimental results. The lateral supporting system of the beam consisted of 4 separate vertical parts assigned as rigid body along the length of the beam, positioned on the edge of the flanges.

As a consequence, the lateral supporting system of the beam had to be re-positioned along the length of the beam with a clearance of 2mm on each side of the beam. This allowed a limited out-of-plane displacement of the beam to take place as in the case of experimental testing.

The final numerical model containing all of these modifications can be seen in Figure 4a) as the force-displacement curve LS3-H0, which closely follows the experimental curve EBF-LF-M-DHTL, with less than 1% difference in values compared to experimental results.

Figure 4 b) shows the resulting deformed shape of the same eccentrically braced frame model. A comparison between the deformed shapes of the dissipative link element at the end of the analysis and at the end of experimental testing can be seen in Figure 3 c) and Figure 3 d) respectively. Similar failure modes can be observed, as the shear of the link web panel is quite obvious and distortion of the dissipative element takes place similarly.

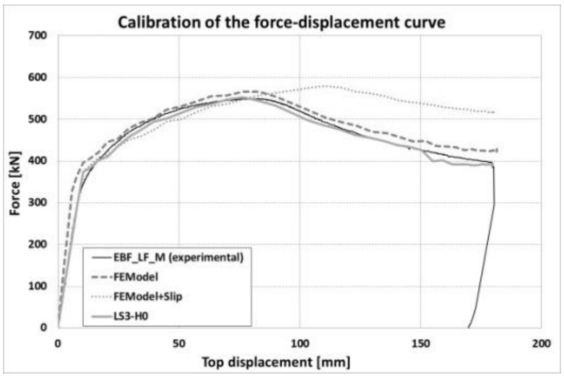

a)

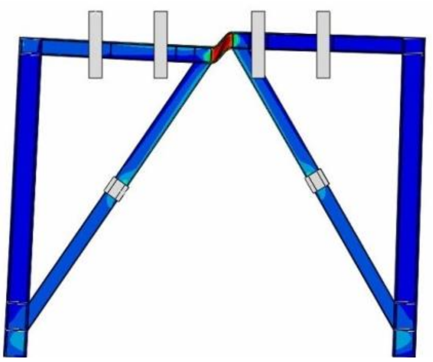

b)

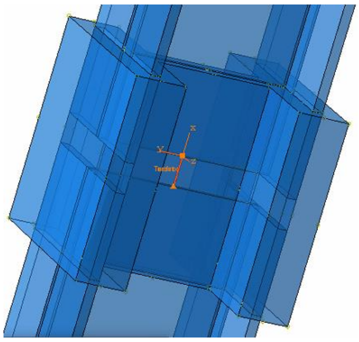

c)

Figure 4. a) Calibration of the force-displacement curve;
b) Deformed shape of calibrated EBF model; c) Detail of slip connector

3. PARAMETRIC STUDY

After the initial calibration was achieved, a parametric study was performed in order to reveal the behaviour of the EBF when considering different parameters such as different link lengths, different configurations for link web stiffening, different link slenderness. Table 1 presents the different numerical models with notations and explanations of the parameters used for each model.

Based on the good initial results which were obtained, an additional model was created using a cyclic loading procedure, in order to quantify the difference in resistance and link distortion in the case of alternant lateral loads.

Table.1 Configurations of analysed EBF models under monotonic loading

Name of FE model	Number of stiffeners	Link section	Link lengthe [mm]	Name of FE model	Number of stiffeners	Link section	Link lengthe [mm]
LS3-H0				LS4-H0	0	HE200A	400
(Reference)	0	HE200A	300	LS5-H0	0	HE200A	500
LS3-H1	1	HE200A	300	LS6-H0	0	HE200A	600
LS3-H2	2	HE200A	300	LS7.5-	0	HE200A	750
LS3-I0	0	IPE240	300	H0	0	IPE240	400
LS3-I1	1	IPE240	300	LS4-I0	0	IPE240	500
LS3-I2	2	IPE240	300	LS5-I0	0	IPE240	600
				LS6-I0	0	IPE240	750
				LS7.5-I0			

3.1. Link length parameterization:

The first analysed parameter was the length of the link, taking into consideration five different lengths. All of the lengths were within the limitations for short link elements, which in this particular case meant a maximum length of 760 mm. For lengths superior to this value, the dissipative element would be subjected to both shear and bending. The lengths which were used were 300, 400, 500, 600 and 750 mm respectively. The models were adapted in order to keep the original bay of 4.5m and changing only the angle of braces in order to accommodate the new link lengths.

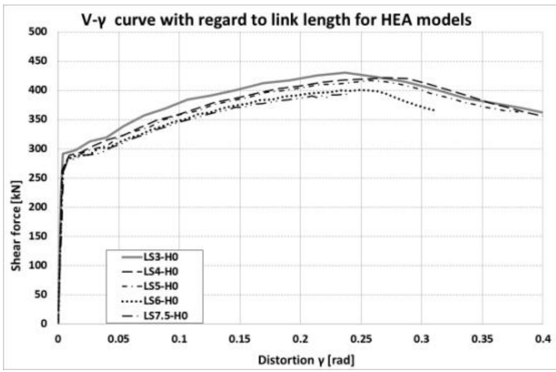

Figure 5. Shear force-distortion curve for different link lengths

Figure 5 shows the response V- γ curves in function of link lengths. A general trend could be observed, where the link length has little influence on elastic and post-elastic ranges: the elastic and ultimate strengths are decreasing with the length, but the difference between the resistances is less than 10% for ultimate and elastic strengths respectively. However, by passing to larger lengths, such as 750

INTERSECTII
INTERSECTIONS
http://www.intersections.ro

mm, the web loses its stability earlier, thus having a limited ultimate resistance and ductility.

This can also be seen in the case of the failure modes, presented in Figure 6. The links with shortest dimensions (300 to 400 mm) are characterized by a global-type shear plasticization while the longer link elements (500 to 750 mm) are characterized by web crippling on sides of the panel, while the other side remaining plain but with high levels of shear stresses.

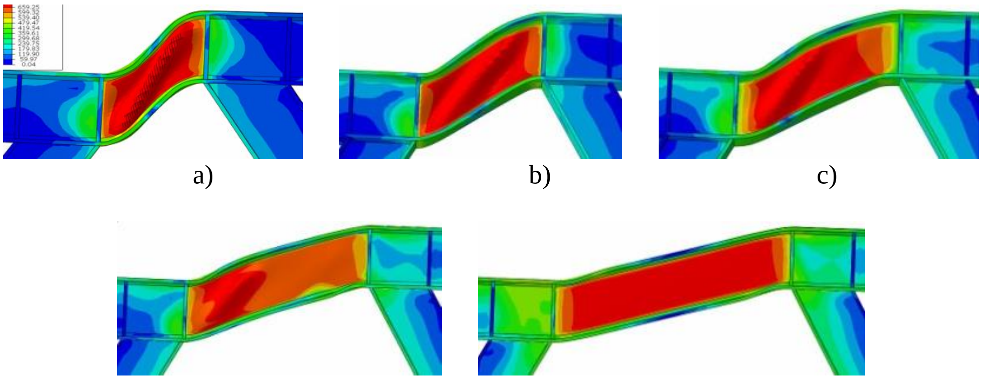

a) b) c)

d) e)

Figure 6. Deformed link shapes at the end of the numerical analysis:
a) 300mm length; b) 400mm length; c) 500mm length; d) 600mm length; e) 750mm length.

3.2. Link web stiffness parameterization:

The second parameter which was analysed was the influence of the stiffness of the link's web on the overall behaviour of the steel frame by comparing three configurations of web stiffening: one model considering no stiffeners on the dissipative link, a second model with one stiffener in the middle of the link (representing the normative solution) and a third model with 2 stiffeners on the link, at equal intervals from the centre and from the end of the link.

According to EN 1998-1 the link elements should be provided with intermediate stiffeners at maximum intervals in millimetres of ($30t_w$-d/5), with t_w being the web thickness and d the height of the cross-section of the link. Consequently, a maximum distance of 155 mm results in the case of an HE200A profile.

Figure 7 shows that the elastic behaviour, initial stiffness and the point of plasticization are practically independent of the number of stiffeners. However, there are important differences in the plastic range: the ultimate resistance of the models' increases with the number of stiffeners and the same happens with the post-elastic stiffness (hardening stiffness).

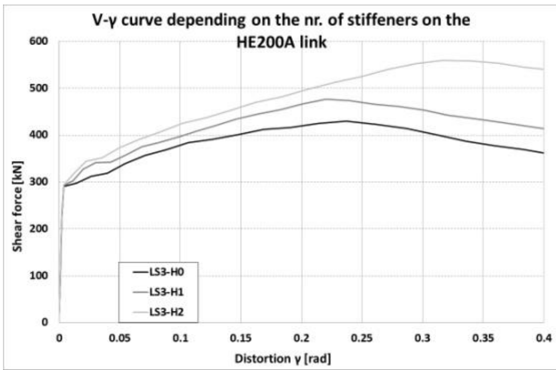

Figure 7. Shear force-distortion curves for different configurations of link web stiffening.

Considering the distortion capacity, all models showed high capacities, up to 0.4rad. The rotation of maximum load shifts from 0.24 to 0.32rad in the case of two intermediate web stiffeners, while for the other two models the difference is visible only in terms of resistance.

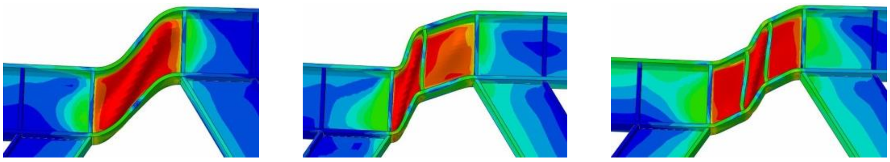

a) b) c)

Figure 8. Deformed shapes of the link elements at the end of analysis:
a) No stiffener; b) One stiffener; c) Two stiffeners.

It could be observed that in both cases additional stiffeners leads to division of the original shear panel into multiple panels, each of these having its own web deformation, as shown in Figure 8. The initial elastic deformations are shared among the panels, but in the post-elastic range the plasticization becomes concentrated in one of the panels, the other contributing only partially to the global deformation.

3.3. Link web slenderness parameterization:

The third parameter, link web slenderness, was taken into consideration by transitioning from an HE200A profile to an IPE240 steel profile for the whole beam. The modification was made by considering the close shear areas of the two profiles, but also the different web slenderness. The value for shear area A_v was computed according to Chapter 6.8 on design and detailing rules for eccentrically braced frames from EN 1998: Part 1. The resulting values for the shear area of the link of 1170mm2 for HE200A and 1427mm2 for IPE240 which represent reduced values for dissipative links, compared to the standard shear area of the two profiles of 1808mm2 respectively 1910mm2 as used for normal gravitational shear verifications. The web slenderness parameter was addressed by changing the profile from HE200A having a nominal web of 7x180 mm with a more slender profile IPE 240 with a web of 6.2x232,9 mm.

The other sections of the frame elements and the global geometrical dimensions remained unchanged. A comparison of the response of the two models is shown in Figure 9 in terms of shear force-distortion curves. Both responses are characterized by a three-linear behaviour:

- an initial elastic behaviour up to plasticization;
- a linear post-elastic hardening branch with important stiffness;
- a discharging branch with similar stiffness as for hardening.

An identical elastic behaviour could be observed when comparing the two responses, with the main difference present in the post-elastic zone: the model with the slender web (IPE profile) showed a slightly smaller maximum resistance, explained by a smaller shear area. This was accompanied by an important reduction in the distortion values corresponding to the maximum load. The local instability appeared earlier in the case of the slender web. For the initial HE200A profile the resistance is slightly higher than for the IPE240 profile, approximately 4%, but at much larger distortion values, of 0.236rad compared to 0.123rad for the slender web.

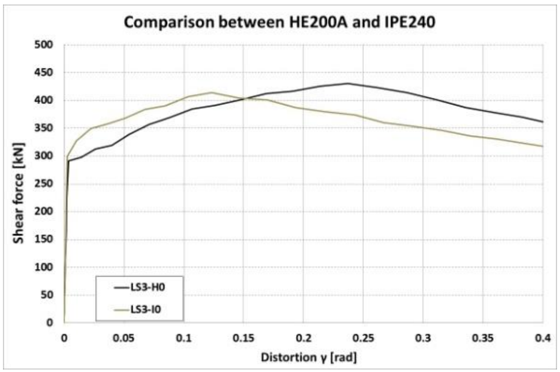

Figure 9. Shear force-distortion curve with regard to the web slenderness of the link element

In both models, a similar shear hinge formed and there was noticeable web crippling due to large horizontal differences of the two lateral sides of the dissipative element. The stress amplitudes outside the link panel were much smaller than those of the internal web itself. The deformed shape of the link elements is presented in Figure 10.

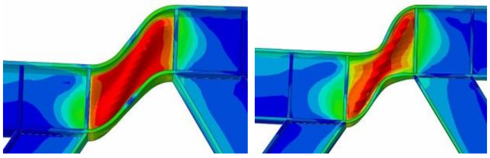

a) b)

Figure 10. Deformed shape of the link element at the end of analysis:
a) HE200A link; b) IPE240 link.

3.4. Monotonic versus cyclic loading:

A final parameter was considered during the study, the influence of cyclic loading compared to monotonic loading on the behaviour of the short dissipative element.

The reference model LS3-H0-M was loaded by displacement control up to 180mm as was done during experimental testing. For the cyclically loaded numerical model, it was necessary to perform a new calibration based on the experimental specimen EBF-LF-C, which was part of the same experimental study described earlier.

The cyclic loading procedure used during experimental testing followed the ECCS loading procedure [13]. Accordingly, three different amplitudes of 0.25Dy, 0.5Dy and 0.75Dy were applied in the elastic range. In the plastic range amplitudes of 1Dy, 2Dy, 4Dy, 6Dy and 8Dy were applied. In all of the above, Dy represents the yield displacement resulted from the interpretation of monotonic tests, in accordance with the ECCS procedure. The load application point is identical to monotonic testing, at the top of the frame and applied in displacement control.

The results from testing can be observed in Figure 11. The experimental response of EBF-LF-C specimen showed a ductile behaviour with good dissipation capacity of the link element with high values of distortion exceeding 150 mrad (Figure 11c). The maximum resistance was of 550 kN, as can be observed in Figure 11b). The failure mode was by alternate shear buckling of the link web panel in positive and negative cycles followed by tearing of the web panel (Figure. 12a).

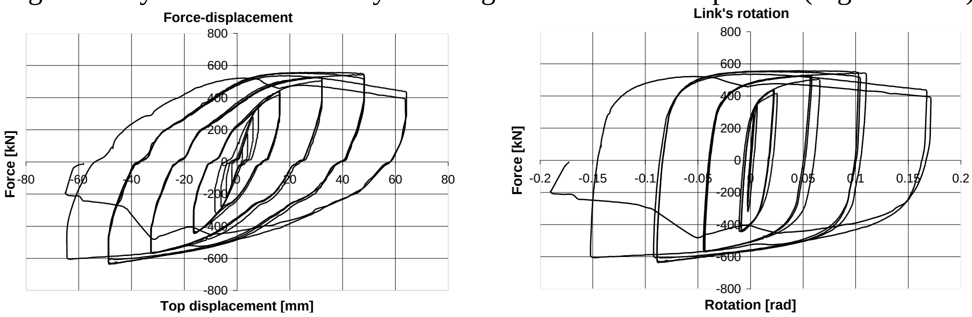

a) b)

Figure 11. a) Force-displacement curve; b) Shear force-rotation curve.

The numerical model LS3-H0-C of the tested frame EBF-LF-C, was created based on the previous numerical model LS3-H0-M by adding certain modifications characteristic for a cyclic loading procedure. The geometry and monotonic material properties of the reference specimen were maintained, but specific cyclic parameters were accounted for:

-Plastic material properties were assigned in order to provide a combined isotropic and kinematic hardening for beam steel material, including the dissipative link element;

-The cyclic material model adopted considered 5 back-stresses in order to accurately model the material behaviour, as suggested by Chaboche [14].

All frame members were modelled using solid finite elements. Hex type elements were used for meshing, considering a sweep technique with a mixed median axis and advancing front algorithms. The finite element size ranged from a fine mesh with 6 mm elements on the dissipative area of the frame (link element and adjacent beam area) to larger element sizes of 15 mm for braces, 20 mm for beam and beam stiffeners and 25 mm for columns and column stiffeners.

The same loading procedure was used as during experimental testing. As in the case of monotonic models, the slip in the brace connections had to be included in the analysis. This meant considering a rigid body element, which allowed the sliding (translation) of the brace and a connector that allows for an elastic spring elongation of the braces, using a behaviour law corresponding to experimentally recorded values. These values were different compared to those recorded during monotonic testing. The change in slip values from monotonic loading to cyclic has led to an increased initial stiffness, and also a better accuracy with the experimental restoring stiffness.

Figure 12 presents the experimental frame top-displacement curves for the experimental response (EBF-LF-C curve) and the finite element calibration (LS3-H0-C curve). The numerical model was considered calibrated when a maximum 6% difference between experimental and numerical values was reached.

ISSN 1582-3024

Adina Vătăman, Adrian Ciutina, Daniel Grecea

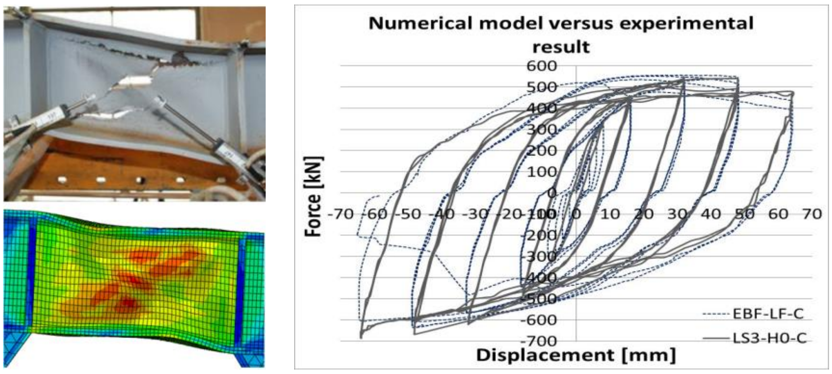

a) b)

Figure 12. a) Deformed shape of the link element at the end of experimental testing of specimen EBF-LF-C; b) Force-displacement calibration curve-experimental versus numerical response.

By comparing the values from monotonic and cyclic analyses it can be observed that the cyclic behaviour introduces a slight limitation in distortion capacity as compared to monotonic responses. However, these values remained higher than the limit value recognised by EN1998-1 of 80 mrad.

As in the case of experimental testing, the cyclic model showed similar values of elastic stiffness to the monotonically loaded model. The rotation of the link element in the case of cyclic loading is smaller than in the case of monotonic loading, but the model reaches higher values resistance for smaller values of link distortion.

4. CONCLUSIONS

The present study was focused on the seismic behaviour of eccentrically braced frames with short steel link elements. Based on a previously existing experimental study on a one-storey specimen, including both monotonic and cyclic loading, two numerical models were developed and calibrated on these experimental results. Further, a parametric study was accomplished based on different parameters: variation of link length, the variation of numbers of vertical intermediate stiffeners on the linked web, different loading procedures.

The study showed that numerically reproducing experimental results is achievable only by carefully defining geometric properties, material laws and testing details, both in the case of monotonic and cyclic analysis. Details such as brace elongations or out of plane displacement of the element, though small (under 2mm) need to be accounted for.

The analysing of different parameters showed interesting results. The increase in the number of stiffeners induced higher shear resistances and improved the overall ductility of the frame, without influencing the elastic stiffness of the system.

The increase in link length (while still remaining in the range of short links) led to smaller maximum resistances and affected the elastic stiffness of the system significantly. Very short links presented a stiffness almost double compared to the links with a length bordering to intermediate length links.

The change of the beam steel profile from HEA to a more slender IPE profile had little influence on the initial elastic domain. The maximum resistance suffered a small decrease, but the major influence was noticeable in terms of distortion levels, which decreased to almost half the initial values for HEA.

In the case of cyclic loading, additional material parameters should be considered in order to control the cyclic behaviour of the entire frame. The Chaboche material model seems to be adequate in accurately modelling the cyclic material response.

The use of a cyclic loading procedure instead of a monotonic one induced both a reduction in maximum shear resistance and distortion capacity of the system. The reduction in shear resistance was up to 5%, while the reduction in distortions was approximately 10%.

However, in all the numerically analysed models the maximum link distortions satisfied the minimum normative requirements of 80 mrad, in accordance with EN 1998-1.

The current study was only focused on analysing the behaviour of short steel elements in eccentrically braced frames and could be broadened to investigate additional parameters, such as different types of stiffeners, longer link lengths exceeding the normative limitations for short link elements, detachable dissipative elements, the influence of the presence of a reinforced concrete slab over the beam, etc. Finite element numerical models seem to be a very accurate solution in predicting such behaviour.

ACKNOWLEDGEMENTS

The research was partially supported by the Sectorial Operational Program Human Resources Development POSDRU/159/1.5/S/137516 financed from the European Social Fund and by the Romanian Government.

References

1. Vayas I., Design of braced frames, *Seismic resistant steel structures*, Chapter 5, CISM Courses and Lectures, 420, 241-288, Springer Verlag Wien GmbH, , 2000

2. Gioncu V., Mazzolani F., *Seismic design of steel structures*, CRC Press Taylor and Francis Group, 2014.
3. European Committee for Standardization – CEN. EN 1998-1, *Eurocode 8: Design of structures for earthquake resistance - Part 1, General rules, seismic actions and rules for buildings*, 2004.
4. Stratan, A., Studiul Comportării Clădirilor Multietajate cu Cadre Metalice Duale Amplasate Ín Zone Seismice, PhD thesis, Universitatea Politehnica Timişoara, 1998.
5. Danku G., Ciutina A., Dubina D., Influence of steel-concrete interaction in dissipative zones of frames: II – Numerical study, *Steel and Composite Structures*, Vol. 15, No. 3 , ISSN 1229-9367, pp: 323-348, 2013.
6. Degée H., Lebrun N., Plumier A., Considerations on the design, analysis and performances of eccentrically braced composite frames under seismic action, *Proceedings of SDSS 2010 Conference –Stability and Ductility of Steel Structures*, 337-344, 2010.
7. Yurisman Y., Budiono B., Moestopo M., Suarjana, M., Behavior of shear link of WF section with diagonal web stiffener of Eccentrically Braced Frame (EBF) of steel structure, *International Journal of. Engineering Science*, 42(2), 103-128, 2010.
8. Okazaki, T., Arce, G., Ryu H.C., Engelhardt M.D., Experimental study of local buckling, overstrength, and fracture of links in eccentrically braced frames, *J. Struct. Eng*. – ASCE, 131(10), 1526-1535, 2005.
9. Danku G., *Study of the development of plastic hinges in composite steel-concrete structural members subjected to shear and/or bending*, Ph.D. Thesis, Politehnica University of Timisoara, 2011.
10. Dassault Systèmes Simulia Corp, Abaqus 6.11-1, 2011.
11. European Committee for Standardisation – CEN. EN 1993-1, 2005. *Eurocode 3: Design of steel structures*.
12. Arasaratnam P., Sivakumaran K.S., Tait M.J., True stress-strain models for structural steel elements, *International Scholarly Research Notices (ISRN) Civil Engineering*, Volume 2011, Article ID 656401, 2011.
13. ECCS TWS 1.3 N.45/86, 1986. Recommended Testing Procedure for Assessing the Behaviour of Structural Steel Elements under Cyclic Loads.
14. Chaboche J.L., A review of some plasticity and viscoplasticity constitutive theories, *International Journal of Plasticity,* 24(10), 1642-1693, 2008.